SSRG International Journal of Electrical and Electronics Engineering
ISSN: 2348-8379/https://doi.org/10.14445/23488379/IJEEE-V12I12P112

Volume 12 Issue 12, 151-162, December 2025

Original Article

Performance Improvement of PMSM Drive System with Bidirectional Battery aware Adaptive Integrated EV Charger

Malleni Omkar[1,2], M. Vijaya Kumar[3]

[1,3]*Department of Electrical & Electronics Engineering, Jawaharlal Nehru Technological University, Anantapur, Anantapuramu, Andhra Pradesh, India.*
[2]*Department of Electrical & Electronics Engineering, Government Polytechnic Anantapur, Andhra Pradesh, India.*

[1]*Corresponding Author : omkarmalleni@gmail.com*

Received: 08 October 2025 Revised: 10 November 2025 Accepted: 12 December 2025 Published: 27 December 2025

Abstract - *This paper presents a bidirectional integrated charger drive system of Electric Vehicles (EVs) that is intended to be efficient, compact, and enhance the safety of batteries. The architecture incorporates a three-phase AC/DC converter having active Power Factor Correction (PFC) as well as a bidirectional buck-boost DC-DC converter, which provides a seamless charging and driving Integration unlike the traditional forms of integrated charger, which recycles the stator windings of the motor as a grid-side filter, which introduces torque ripple, acoustic noise, and complex control. The proposed design has a Permanent Magnet Synchronous Motor (PMSM) as the only propulsion, which will minimize the hardware and maximize the driveability. It consists of the adaptive charging strategy approach based on the real-time feedback of the temperature of the battery and State Of Charge (SOC), supplemented by a first-order thermal model, allowing fast charging with enhanced safety and protection of the battery. The simulation findings show a unity power factor, high efficiency of 97.2%, low Total Harmonic Distortion (THD) of 1.62%, smooth conversion between A Constant Current (CC) and Constant Voltage (CV) charging system, in addition to improved performance of the motor operating in drive mode. The proposed architecture combines adaptive battery-aware control with the conventional utilisation of PMSM-based propulsion to offer a high-performance and scalable way for next-generation electric vehicles.*

Keywords - *Integrated charger, Electric Vehicle (EV), adaptive CC–CV charging, Battery aware, Permanent Magnet Synchronous Motor (PMSM).*

1. Introduction

With the rise in the use of Electric Vehicles (EVs), there has been a high demand for onboard chargers, which are compact, high-efficiency, and cost-effective. The typical implementation of the conventional EV powertrains is to use separate converters to charge the battery and propulsion, leading to a 20 -30% increase in the overall mass, cost, and volume of the onboard charger. These extra parts not only make the system more complex, but also influence the flexibility and overall efficiency of the vehicle [1, 2]. To overcome these difficulties, studies have devoted more attention to integrated charger-drive systems, where the same hardware is used in propulsion and charging, leading to a better utilisation of energy and reducing the size of the system [3, 5]. However, the practical realisation of integrated charger–drive systems introduces new challenges related to torque disturbance, control coupling, and battery safety. In particular, sharing propulsion hardware during charging can adversely affect motor performance and complicate control coordination, especially in high-power electric vehicle applications. Several integrated charger topologies have been suggested in the literature, most of which are concerned with the way stator motor windings are reused during the charging process, and explored motor-winding-based integration, in which the windings of the motors are employed as a part of the charging filter [6, 8]. While such designs effectively reduce the number of components, they introduce torque ripple and electromagnetic interference. To overcome these drawbacks, torque cancellation methods have been proposed [9-11], but they have complex control coordination between motor and charging operations. These effects degrade drive smoothness, increase mechanical stress, and limit scalability for high-power electric vehicle operation.

In contrast, other literature has proposed multiphase and special motor-based topologies to achieve partial hardware sharing while minimising coupling effects. To improve charging efficiency, different configurations have been

proposed that utilise additional motor windings or modified inverter connections [12, 13]. Although these architectures demonstrate improved power transfer capability, they often require non-standard machine designs, complex switching arrangements, and additional magnetic components, which increase design cost and reduce compatibility with conventional PMSM-based propulsion systems.

Despite these advances, most previous studies mainly focused on power conversion and paid little attention to real-time battery condition monitoring, and it will be shown that most integrated charger–drive systems lack SOC and temperature-feedback-based adaptive control [14, 15], leading to sub-optimal charging profiles. Recent studies have also focused on battery-aware control and real-time monitoring to enhance the safety and lifespan of the batteries and also emphasized the need for state-of-charge (SOC) and thermal feedback integration during charging to prevent overvoltage, overheating, and accelerated degradation [16, 17]. However, the control strategies have been proposed in isolated charger systems, but have not been effectively integrated within bidirectional onboard architectures that handle both charging and propulsion modes.

From the above discussion, it is evident that a clear research gap exists in the development of integrated charger–drive systems that simultaneously ensure torque-disturbance-free propulsion and battery-aware adaptive charging. Existing integrated architectures largely neglect real-time SOC and thermal feedback. A unified bidirectional on-board solution that integrates conventional PMSM propulsion with adaptive, battery-protected charging remains insufficiently addressed.

To address the aforementioned research gaps, this article outlines an adaptive CC -CV (constant-current/ constant-voltage) controller with a bidirectional converter architecture that eliminates the motor winding utilized as a filter. The suggested system will also guarantee high efficiency, decreased harmonic distortion, and increased battery protection since the battery parameters are adjusted dynamically in reaction to instantaneous SOC and temperature feedback. Moreover, the architecture has a smooth changeover between charging and driving modes, thus enhancing the reliability of the system, energy utilisation, and compactness of the hardware compared to existing systems.

The proposed work novelty lies in the simultaneous Incorporation of a battery-aware adaptive charging strategy within a bidirectional charger–drive architecture while preserving a conventional PMSM propulsion system. Unlike existing integrated chargers that reuse motor windings or require non-standard machines, the proposed system completely decouples propulsion from charging hardware, thereby eliminating torque ripple and control coupling. Furthermore, in contrast to prior battery-aware charging methods limited to standalone chargers, this work embeds real-time thermal feedback and SOC directly into a bidirectional on-board charger that supports both charging and driving modes using shared power electronics.

2. Methodology

2.1. System Topology

Figure 1 shows an integrated bidirectional charger and propulsion topology that enables both grid-connected charging and motor-driven vehicle operation by selectively controlling switches K_1 and K_2. During charging mode, K_1 is closed, and K_2 is opened, connecting the three-phase grid to the AC/DC bidirectional converter through the inductors. The inductors act as input filters to suppress current ripple and harmonics, ensuring power quality and controlled energy transfer from the grid.

The bidirectional AC/DC converter converts the grid AC supply into a stable DC-link voltage (Vdc), which is further conditioned by the buck-boost converter, which is used to regulate charging current delivered to the battery. During driving mode, K_2 is closed, and K_1 is opened, isolating the grid and driving the PMSM via the same AC/DC converter, which now functions as an inverter. The battery delivers DC power that is boosted by the buck-boost converter to keep the stable voltage of the DC-link. The inverter then transforms this DC power into three-phase AC to operate the PMSM, providing the required torque for vehicle propulsion. This switching arrangement allows the power converter to be shared between charging and driving operations, reducing system size, weight, and cost while enabling seamless bidirectional energy flow.

2.2. Mathematical Analysis of a Bidirectional AC/DC Converter

Based on Figure 1, the system model Equations can be denoted as [18].

$$\begin{aligned} v_a &= L\frac{di_a}{dt} + Ri_a + u_{an} + u_{no} \\ v_b &= L\frac{di_b}{dt} + Ri_b + u_{bn} + u_{no} \\ v_c &= L\frac{dic}{dt} + Ri_c + u_{cn} + u_{no} \\ c\frac{dv_{dc}}{dt} &= i_{dc} - i_L \end{aligned} \tag{1}$$

where Uno is the voltage between N and O. The Switching function S_k is 1 when the switch is in the on state and zero when it is in the off state. Thus, U_k may write as,

$$\begin{aligned} u_k &= u_{kn} + u_{no} = s_k u_{dc} + u_{no} \qquad (k = a, b, c) \\ v_a &= L\frac{di_a}{dt} + Ri_a + v_{dc}[s_a - \tfrac{1}{3}(s_a + s_b + s_c)] \\ v_b &= L\frac{di_b}{dt} + Ri_b + v_{dc}[s_b - \tfrac{1}{3}(s_a + s_b + s_c)] \\ v_c &= L\frac{di_c}{dt} + Ri_c + v_{dc}[s_c - \tfrac{1}{3}(s_a + s_b + s_c)] \\ C\frac{dv_{dc}}{dt} &= i_a s_a + i_b s_b + i_c s_c - i_L \end{aligned} \tag{2}$$

The stationary a,b,c frame can be represented as α, β a frame by using the Clark transformation as:

$$\begin{aligned} v_\alpha &= L\frac{di_a}{dt} + Ri_a + s_a v_{dc} \\ v_\beta &= L\frac{di_b}{dt} + Ri_b + s_b v_{dc} \\ c\frac{dv_{dc}}{dt} &= \frac{3}{2}(i_a s_a + i_b s_b) - i_L \end{aligned} \quad (3)$$

The quantities in the α, β frame can be converted to the d–q reference frame using Park's transformation

$$\begin{aligned} v_d &= L\frac{di_d}{dt} + Ri_d - w_o L i_q + s_d v_{dc} \\ v_q &= L\frac{di_q}{dt} + Ri_q + w_o L i_d + s_q v_{dc} \\ c\frac{dv_{dc}}{dt} &= \frac{3}{2}(i_d s_d + i_q s_q) - i_L \end{aligned} \quad (4)$$

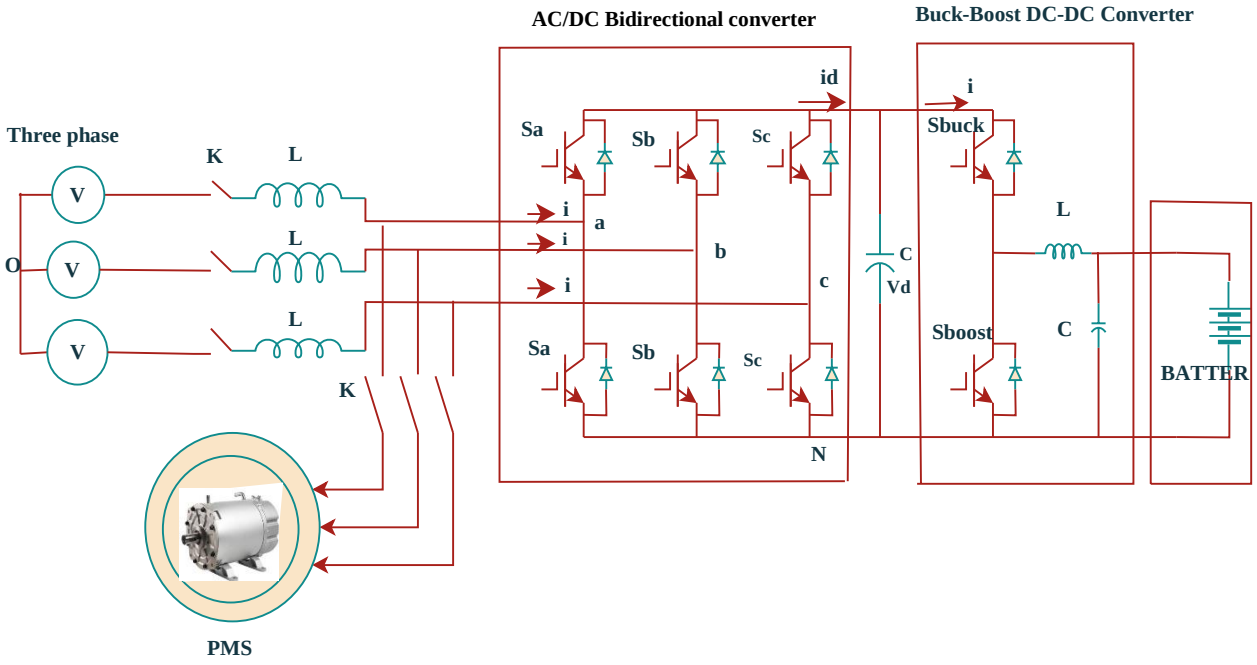

Fig.1 Integrated bidirectional charger

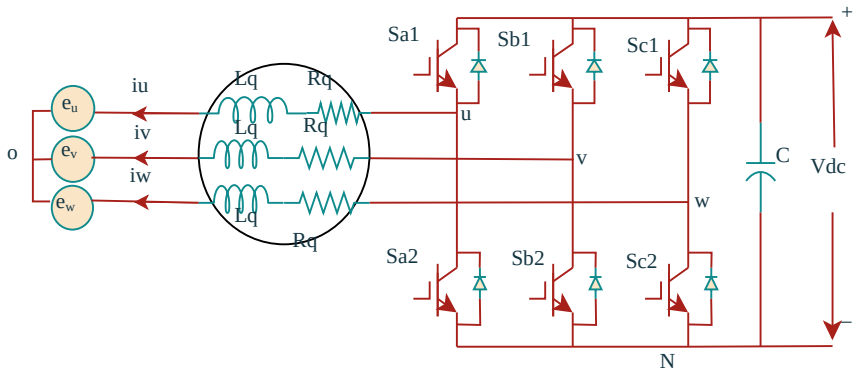

Fig. 2 Equivalent circuit of PMSM in driving mode

2.3. Mathematical Modelling of PMSM

Figure 2 depicts the equivalent PMSM circuit in propulsion mode, which illustrates the interaction between the stator and inverter. The stator windings of phases u_u, v_v, and w_w are modeled using the series combination of resistance Rq and inductance Lq, which represent copper losses and magnetic energy storage, respectively.

The back electromotive forces, eu,ev, ew, arise from rotor motion and are proportional to the rotor speed and magnetic flux. The voltage Vdc transforms into a three-phase AC output by the inverter to supply the stator windings, producing torque. The stator voltages of PMSM are given by:

$$\begin{bmatrix} v_u \\ v_v \\ v_w \end{bmatrix} = \frac{d}{dt}\begin{bmatrix} \psi_u \\ \psi_v \\ \psi_w \end{bmatrix} + R_q \begin{bmatrix} i_u \\ i_v \\ i_w \end{bmatrix} \quad (5)$$

The flux linkages are given by

$$\begin{aligned} \psi_u &= L_u i_u + M_{uv} i_v + M_{uw} i_w + \psi_{fu} \\ \psi_v &= L_v i_v + M_{uv} i_u + M_{vw} i_w + \psi_{fv} \\ \psi_w &= L_w i_w + M_{vw} i_v + M_{uw} i_u + \psi_{fw} \end{aligned} \quad (6)$$

In the frame of reference d-q, the voltage equations of the PMSM are represented as follows.

$$\begin{aligned} v_d &= R_q i_d + \frac{d}{dt}\psi_d - w_e \psi_q \\ v_q &= R_q i_q + \frac{d}{dt}\psi_q + w_e \psi_d \end{aligned} \quad (7)$$

The electromagnetic torque is,

$$T_{em} = P_n(\psi_f i_q + (L_d - L_q) i_d i_q) \quad (8)$$

3. Control strategy

3.1. Control Technique during Charging

Figure 3 illustrates the controller for the grid-connected bidirectional charging system, which combines grid-side and battery-side control loops. The reference angle θ generated by the Phase-Locked Loop (PLL) used for the transformation of grid currents into the frame of d–q, enabling decoupled control and the generation of Vd and Vq components. These voltage components are then converted back to a phase system and supplied to the PWM, which drives the switches of the bidirectional AC/DC converter. On the DC side, an adaptive controller adjusts the reference voltage and current based on SOC and battery temperature, ensuring smooth CC–CV transition for effective and safe charging.

3.2. Control Strategy during Propulsion

The controller coordinates battery discharging to drive the PMSM through the bidirectional converter, as shown in Figure 4. In drive mode, the battery supplies power, which is regulated by the buck–boost converter to maintain the required DC-link voltage. The AC-DC bidirectional converter works similarly to an inverter, transforming the DC link voltage to three-phase AC to the motor.

The controller of the speed deviates from the desired speed Nref and the real speed measured by the encoder and produces reference q-axis current(Iqref) to produce the torque and flux regulation by the d-axis current (Idref). The three-phase currents that were measured were changed to a d-q reference frame to be accurately regulated by the current controllers. The three-phase signals are again converted into the controller outputs and fed to the PWM, which drives the switches on the AC-DC converter. This Integrated control ensures an efficient conversion from battery to the motor and stabilises DC link voltage, precise regulation of the torque, and smooth propulsion in drive mode.

3.3. Buck-Boost DC-DC Converter Adaptive Controller

Figure 5 shows the adaptive control, which dynamically alters the mode of operation depending on real-time SOC and temperature of the battery. Based on feedback, the controller produces adaptive current (Iad) and voltage (Vad), which are compared to the reference current and voltage. PI controllers are used to regulate the resulting errors to properly track the charging profile.

The system operates at a constant current mode up to the SOC reaches 80% and then at a constant voltage mode when the SOC exceeds the threshold value (80%). A mode selection block allows a smooth change between the two modes, and the controller's output drives the DC-DC converter to manage the amount of power sent to the battery.

The first-order thermal differential equation governs the temperature variation of the battery as,

$$C_{th}.\frac{dT}{dt} = I^2.R\frac{T - T_{amb}}{R_{th}}_{int} \quad (9)$$

Figure 6 shows the battery thermal model, which predicts the temperature increase of the battery taking into consideration internal heat generation and Ambient temperature. The current used in charging causes Joule's losses equal to I^2R_{int}, where R_{int} is the battery's internal resistance. The thermal resistance (Rth) describes heat exchange with the surroundings, whereas Cth is thermal capacitance that describes heat storage in the batteries. The net heat flow is calculated by integrating the time to predict the transient battery temperature, which is important in the thermal assessment of the battery in charge and drive mode.

Figure 7 illustrates a strategy of adaptive charging that controls the charging of the battery in relation to the state of charge and temperature. This begins with a monitoring of these parameters to identify the appropriate mode of charging. With a SOC below 80%, the system works in Constant Current (CC) mode and provides the maximum allowable current (I=Imax) to allow the system to charge quickly.

Should the temperature of the battery attain its pre-determined threshold, the current is correspondingly reduced ($I = I \times \alpha$) to avoid excessive heat. When SOC is above 80%, the controller switches to Constant-Voltage (CV) mode, keeping the battery voltage constant at the highest allowable voltage (V = Vmax) as the charging current smoothly drops. The SOC is constantly monitored, and when it reaches 100%, the charging is interrupted, which ensures safe, effective, and reliable operation of the battery.

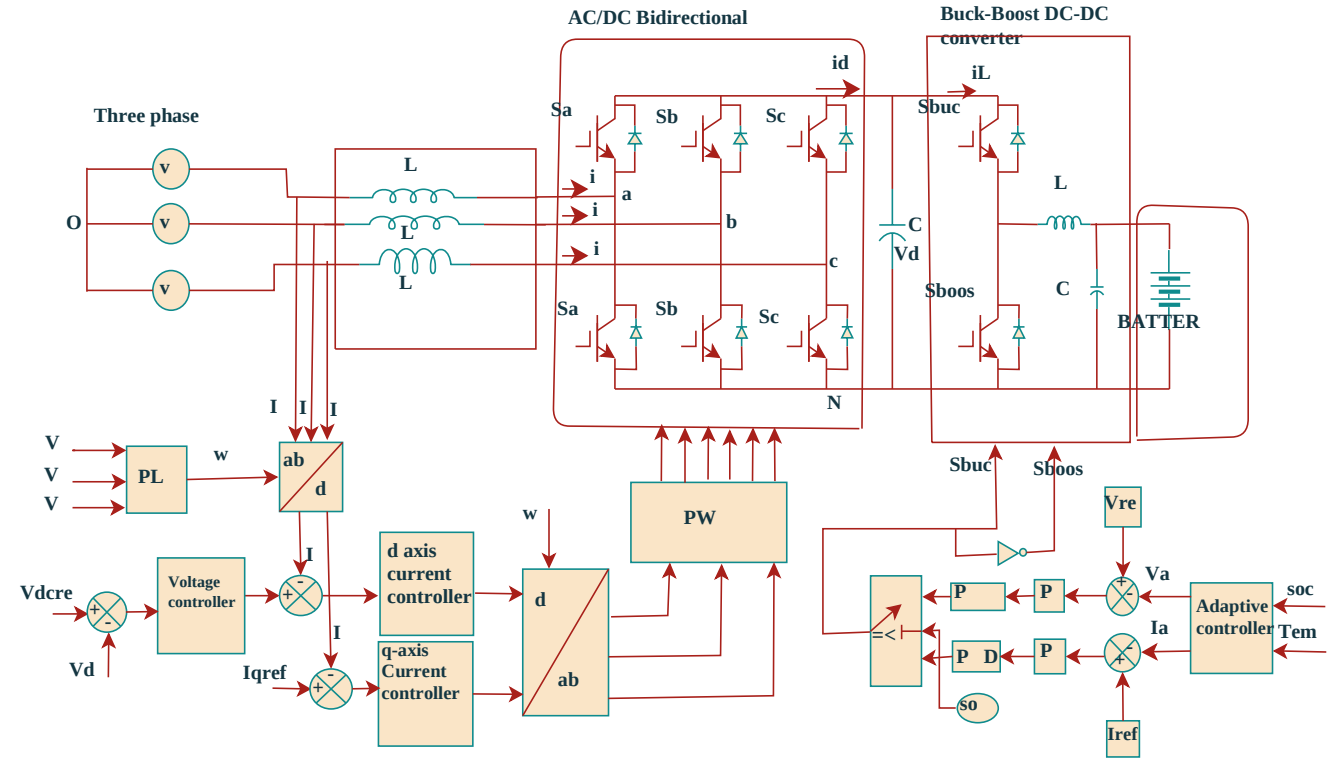

Fig. 3 Control technique block diagram during charging

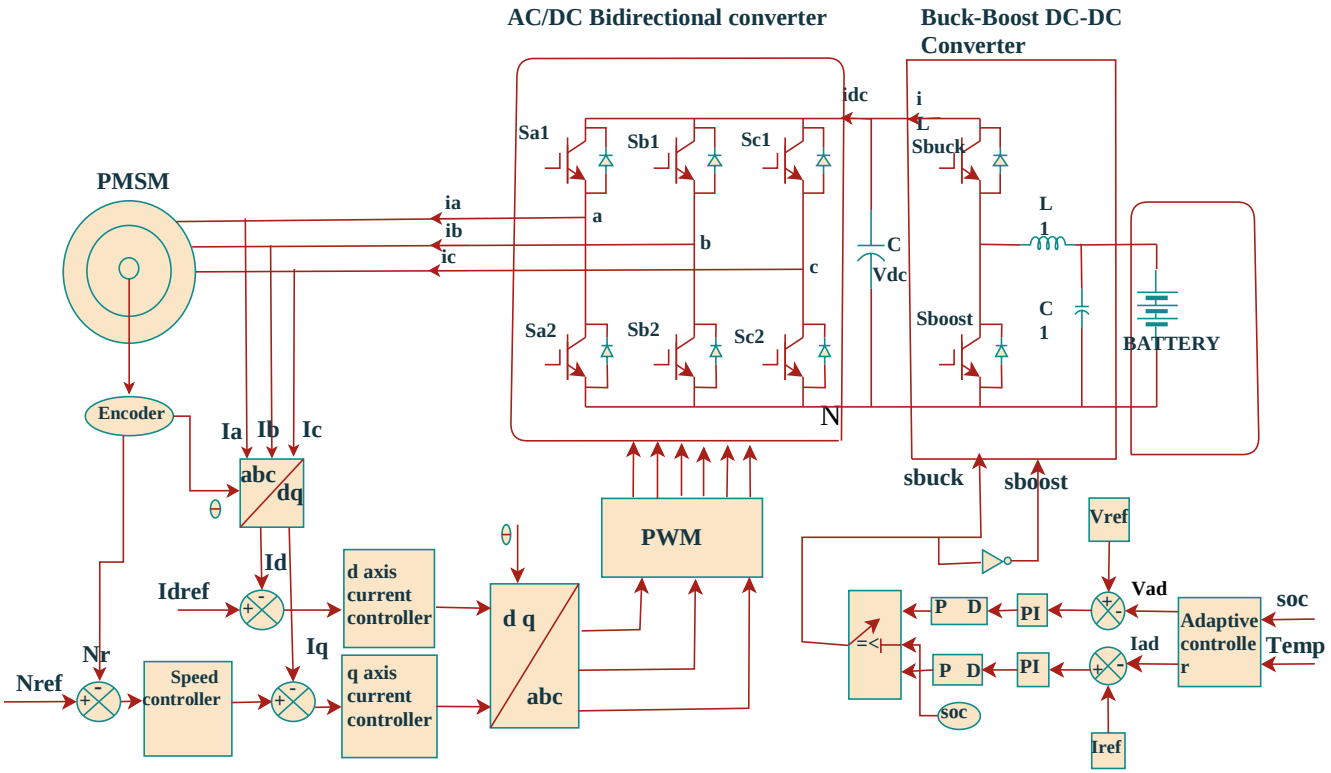

Fig. 4 Control strategy block diagram during driving mode

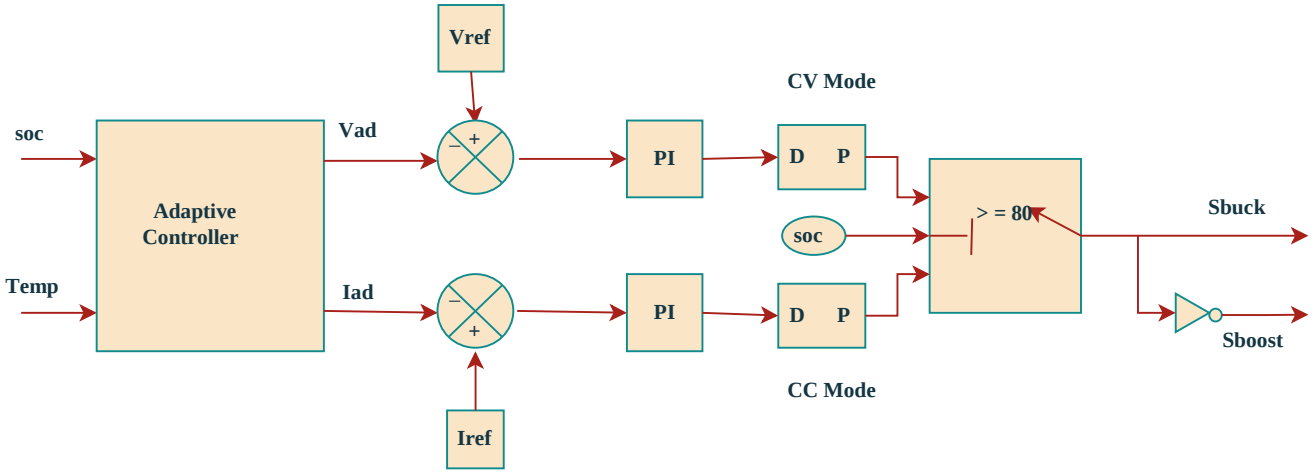

Fig. 5 Block diagram of the adaptive controller

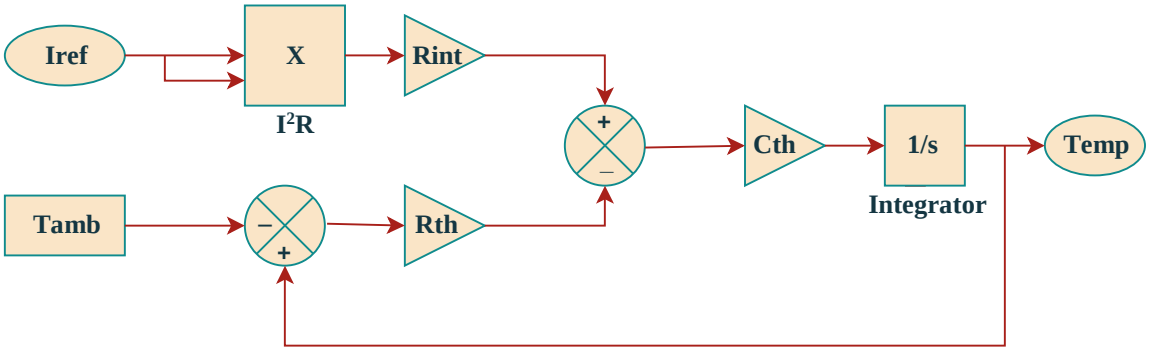

Fig. 6 Thermal model of the battery

4. Simulation Results

4.1. Performance of the Integrated Bidirectional Charger in Charging Mode

Table 1 presents the key parameters used in the MATLAB/Simulink implementation of the proposed integrated charger–drive system. The simulation is performed using a three-phase 325 V, 50 Hz grid with a 10 kHz switching frequency, maintaining an 800 V DC-link supported by a 10 mH input filter and a 5600 µF capacitor to ensure stable operation and low voltage ripple. The connected battery is rated at 400 V and 40 kWh, charged with a maximum current of 25 A, where the control shifts from cc to cv mode at 80% SOC. The model also accounts for an internal battery resistance of 0.1 Ω and maintains a threshold temperature of 45 °C to assure efficient and thermally safe charging performance.

Table 1. System and battery parameters

Parameter	Value
Grid Voltage	325 V
Grid current	21 A
Grid Frequency	50 Hz
Switching Frequency	10 kHz
DC-Link Voltage	800 V
Inductance of the Filter	10 mH
DC link Capacitance	5600 µF
Battery Voltage	400 V
Battery Current	25 A
Capacity of the battery	40 kWh
Initial SOC	20%
SOC Threshold (CC→CV)	80%
Internal Resistance of the Battery	0.1 Ω
Threshold Temperature	45 °C

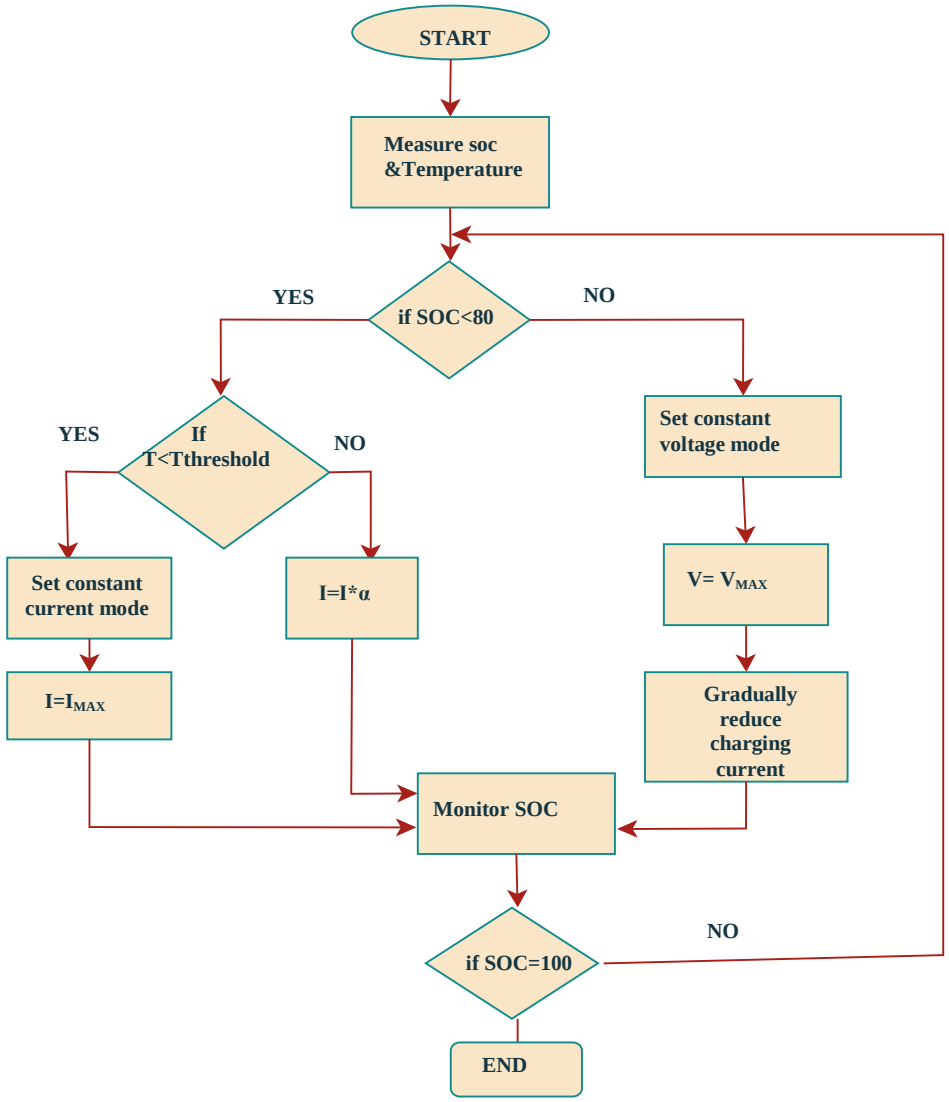

Fig. 7 Flowchart of an adaptive controller

Figure 8(a) illustrates that the three-phase voltages are balanced and sinusoidal with a peak value of 325 V, and Figure 8(b) shows the currents with a peak value of approximately 21 A. The operating voltages are also synchronized with the currents, which implies that the operation is a unity power factor, which means that the grid is stable and the harmonic distortion is minimum. Figure 8 (c) indicates that the battery voltage will vary slowly at the constant-current charging stage, and during constant voltage phase the voltage is constant and has a value equal to 400 V. Figure 8 (d) shows that the current flowing through the battery remains constant and the current is approximately 25A during constant-current charging stage and at the constant voltage phase current steadily reduces to a few amperes as the battery attains full state-of-charge.Figure 8(e) indicates that the SOC rises gradually to about 100% during the charging phase from an initial value of 20%. Figure 8(f) indicates a stable DC-link voltage of 800 V and shows the effective regulation during conversion operation. Figure 8(g) gives the value of the Grid current THD of 1.62%. During charging mode, the system exhibits efficient power transfer and provides consistent charging performance.

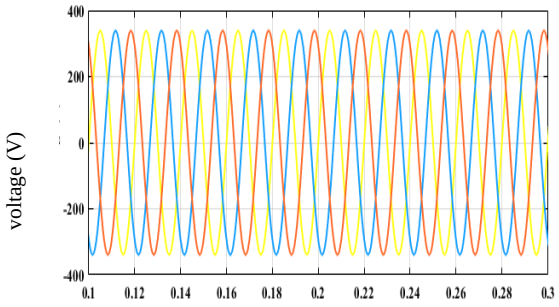

(a)

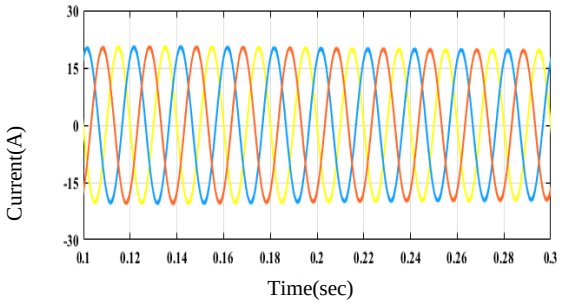

(b)

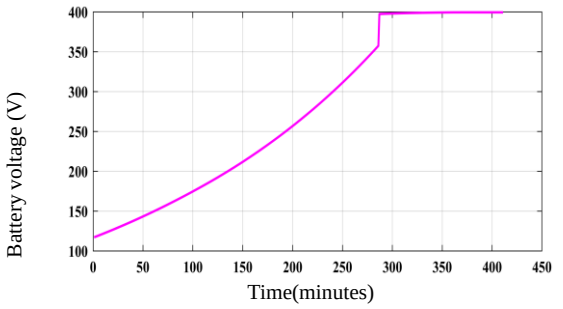

(c)

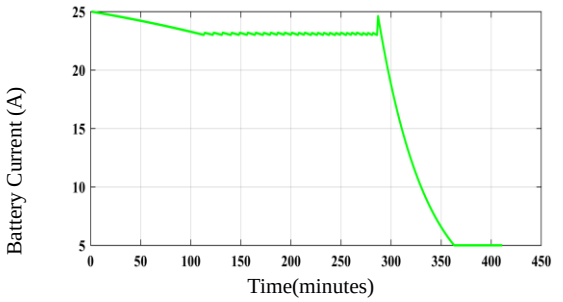

(d)

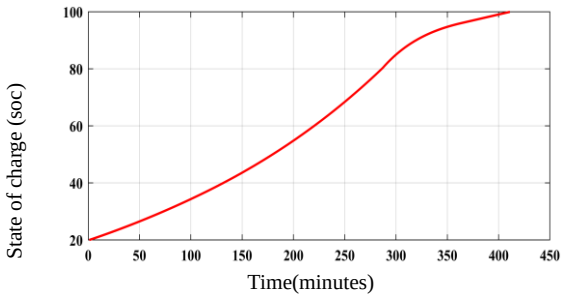

(e)

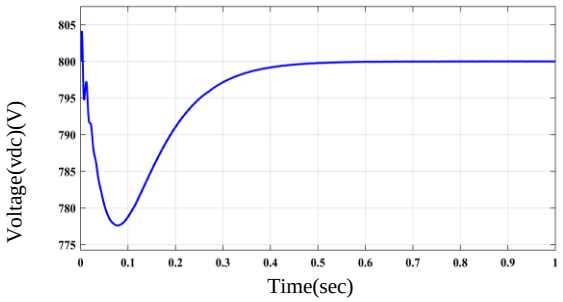

(f)

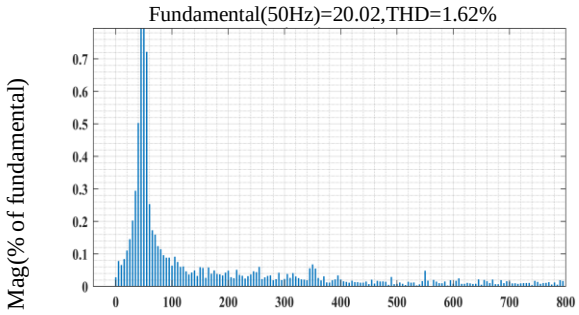

(g)

Fig. 8 Performance of the integrated bidirectional charger during charging, (a) Grid voltage, (b) Grid current, (c) Battery voltage, (d) Battery current, (e) State of charge, (f) Voltage (vdc), and (g) THD of grid current.

4.2. Performance during Driving Mode

Table 2 shows the PMSM motor parameters used in the MATLAB/Simulink model, featuring a 12 kW rated power, 30 N-m torque, 3000 rpm speed, and a four-pole configuration for traction operation.

Table 2. Parameters of PMSM

Parameter	Value
Rated power	12 KW
Rated torque	30 N-m
Rotor speed	3000 rpm
No.of poles	4

Figure 9(a) depicts Battery voltage decreases gradually from approximately 415 V to around 120 V over the discharge duration. Figure 9(b) shows the battery current discharging constantly at approximately 25 A throughout the discharging period. Figure (c) illustrates that SOC decreases progressively from an initial value of 100% to about 20% over the discharge duration. Figure 9(d) represents the voltage (vdc) response during discharging, where the voltage is regulated steadily at 800 V throughout the operation. The minimal ripple and absence of fluctuations indicate effective regulation, confirming stable power transfer during driving operation.

Figure 9 (e) depicts motor Currents that are balanced and sinusoidal with a peak magnitude of ±35 A**.** Figure 9(f) shows that the torque initially exhibits a transient fluctuation as the system starts up and then stabilises to a nearly constant value of 30 N-m, indicating stable performance of the drive.

Figure 9(g) represents q-axis current increases rapidly to a value of 35 A, governing the electromagnetic torque production, while the d-axis current settles close to zero, indicating effective decoupling of the flux and torque components. Figure 9(h) shows the motor speed, which runs at 3000 rpm throughout the operation. Overall, during driving mode, the system exhibits stable operation with efficient power transfer and consistent motor performance.

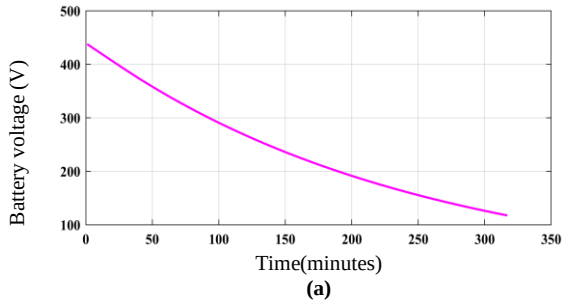

(a)

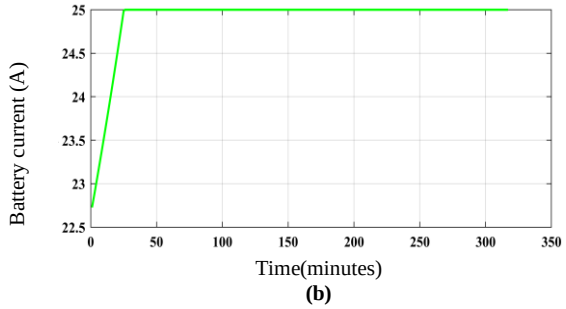

(b)

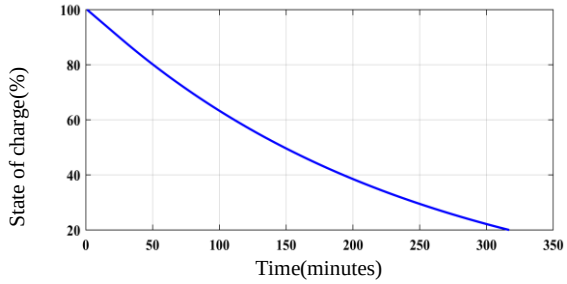

(c)

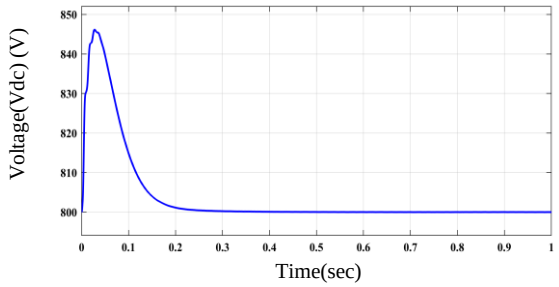

(d)

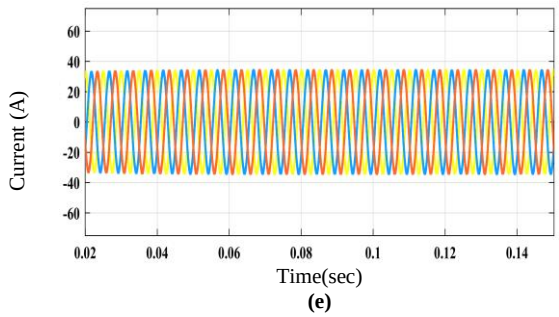

(e)

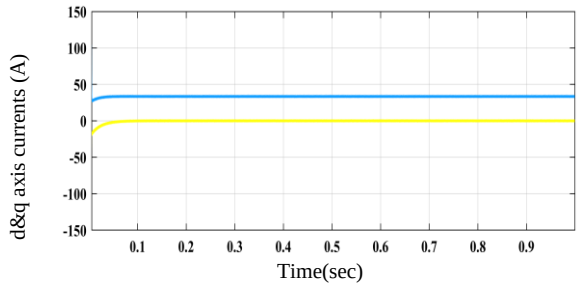

(f)

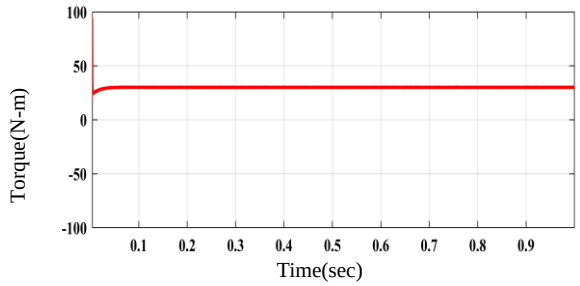

(g)

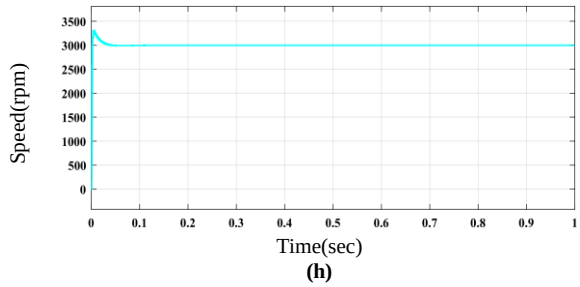

(h)

Fig. 9 Performance of the integrated bidirectional charger during driving: (a) Battery voltage, (b) Battery current, (c) State of charge, (d) DC link voltage, (e) Stator current, (f) Direct and quadrature axis currents, (g) Torque, and (h) Speed.

5. Analysis and Discussion

The integrated bidirectional charger drive system has excellent performance in terms of quality of power, efficiency, and the compact size of hardware over the currently existing integrated topologies. In contrast to traditional motor-winding-based architectures, which are afflicted by torque ripple, harmonic distortion, and control coupling, the proposed design uses a decoupled three-phase AC/DC converter with an active (PFC)-based and bidirectional buck-boost DC-DC converter, which maintains smooth operation in both charging and driving modes. The system stabilizes at 800 V DC link voltage and charging efficiency of 97.2 %, with the grid current THD of 1.62%, which is excellent harmonic suppression and operating unity power factor. By incorporating an adaptive CC-CV control algorithm, which is backed by SOC and temperature real-time feedback, ensure safe and efficient charging with less stress to the battery and higher reliability. Also, the removal of motor-winding filters and isolation Transformers reduces hardware volume, size,

and weight. Table 3 contrasts the proposed integrated charger drive system with existing configurations. The comparison shows that the proposed design outperforms previous topologies in the essential performance parameters like THD, efficiency, elimination of torque ripple, and thermal awareness. Also, earlier literature lacks feedback on battery health and thermal monitoring and is less flexible for real-world applications. These features are incorporated into the proposed charger as a unique control framework, which offers greater safety, longevity, and adaptability of the system that stores energy. The improved performance of the proposed system compared to existing integrated charger topologies that rely on motor-winding reuse or multiphase machines [6–13], the proposed system achieves torque-disturbance-free operation without requiring additional motor windings, torque cancellation algorithms, or special machine designs. Earlier studies primarily evaluate power quality and converter efficiency, whereas the present work extends the comparison by incorporating battery state-of-charge and thermal dynamics into the control framework. This integrated consideration enables safer and faster charging while maintaining stable propulsion performance, which is not simultaneously addressed in existing charger-drive systems.

6. Conclusion

The proposed bidirectional integrated charger drive system offers a volume-efficient, cost-effective, and compact solution that meets the needs of efficient on-board charging and high-performance propulsion in electric vehicles. The proposed design has a compact architecture, high efficiency, low Total Harmonic Distortion(THD), and consistent motor operation without involving motor windings as filters or non-standard topologies of the motor, and it combines a bidirectional three-phase AC/DC converter and a buck-boost DC-DC converter. The main advantage of the suggested design is that it provides propulsion with the help of a conventional PMSM, eliminating the torque ripple, harmonic distortion, and other complications of control complexity in the designs that reuse the windings of the motors as filters. The proposed bidirectional integrated charger drive system is a low-volume, economical, and compact solution that meets the requirements of efficient on-board charging and high-performance propulsion in electric vehicles. The overall benefit of the proposed design is that propulsion is achieved by means of a standard PMSM, which eliminates the torque ripple, harmonic distortion, and other hassles of the complexities of the control in the designs that reuse the windings of the motors as filters. Real-time SOC and thermal feedback assistance to the adaptive CC-CV controller of the system enables dynamic adjustment of the charging profile of the system to ensure safe, fast charging, enhanced battery life, and reduced operational stress. The optimization of the battery protection is incorporated with a first-order thermal model to precisely predict the temperature rise. Simulation studies reveal that the proposed system can achieve a high efficiency of 97.2%, a low THD of 1.62%, smooth transitions between the constant control and constant voltage modes, and a constant DC link voltage of 800 V and a lighter and less costly powertrain solution as compared to the earlier integrated chargers. The integration of reduced hardware and battery-ware adaptive control makes the proposed system a high-performance, scalable, and practical solution to the future EV platforms, aiming at increased efficiency, decreased size, cost, and enhanced safety.

Table 3. Comparison of the existing charger with the proposed Integrated charger

Ref.	Motor Type/ Topology	Filter / Power Stage Strategy	Torque Ripple, Noise and Vibration	Control Complexity	Battery SOC /Thermal Monitoring	Hardware Size& Efficiency	Grid Current THD (%)
[6]	3-Phase Induction Motor	Stator windings reused as a grid filter	High torque ripple and mechanical stress during charging	Moderate (dual-frame current control)	Not included	Compact hardware but limited reliability	3.72
[10]	IPMSM	Motor windings as filter	Significant torque vibration and acoustic noise	High (harmonic mitigation required)	Not included	Reduced passive components but complex control	3.5
[8]	Split-phase machine	Motor winding reused as a filter	Pulsating torque and electromagnetic vibration persist	Requires harmonic suppression	Not included	Compact but not optimised for high-power operation	3.32
[12]	5-Phase Hybrid-Excitation FSPM	Multiphase topology with torque cancellation	Low torque ripple during charging	High (multiphase decoupling)	Not included	Bulky drive and charger; higher cost	2.7

[13]	6-Phase PMSM with galvanic isolation	Dedicated inductors and dual converter stages	Torque ripple minimised	High (additional isolation and loops)	Not included	Larger and heavier system	2.5
[11]	3-Phase PMSM with torque-cancellation control	Conventional motor with enhanced control	Low torque ripple (parameter-dependent)	High (computational burden)	Not included	Compact; requires accurate parameter tuning	2.5
Proposed Work	3-Phase PMSM	External filter with active PFC, bidirectional buck–boost DC-DC converter	No torque ripple, smooth and quiet operation	Moderate uses FOC and adaptive CC–CV control	Integrated SOC and temperature feedback for adaptive charging	Compact, high-efficiency, thermally safe operation	1.62

6.1. Limitations and Future Scope

The proposed system validation is currently limited to MATLAB/Simulink simulations. Real-time performance, such as parameter variations and EMI effects, needs to be tested experimentally. While the existing PI-based control is stable, it may not be adaptive under dynamic grid or temperature conditions, and it can be enhanced in the future using advanced control schemes. The thermal model also assumes homogeneous heat distribution. The future scope of this research includes the hardware implementation of the proposed system with the use of a real-time Hardware-In-the-Loop (HIL) platform. The Future research will involve the incorporation of machine learning-based battery state prediction to improve system flexibility in the face of different grid and thermal conditions. The design will be extended to a multi-port architecture to enable multiple (V2X) coordinated operations, which will be explored to improve the scale and energy management in smart grid environments.

Abbreviations

Symbol	Parameter	Unit / value
v_a, v_b, v_c	Grid side voltages	V
i_a, i_b, i_c	Grid side currents	A
L	Circuit Inductance	mH
R	Circuit Resistance	Ω
Vdc,	Voltage across the DC link	V
idc	Current flow through the DC link	A
C	Capacitance of the DC link	µf
U_{an}, u_{bn}, u_{cn}	Converter side voltages	V
Sa,Sb,Sc	Switching functions	0 or 1
e_u, e_v, e_w	Stator voltages of the motor	V
i_u, i, i_w	Stator currents of the motor	A
ψ_u, ψ_v, ψ_w	Stator flux linkages	Wb
L_u, L_v, L_w	stator winding Self inductances	H
M_{uv}, M_{vw}, M_{uw}	stator winding Mutual inductances	H
w_e	Angular velocity of the rotor	rad/s
Cth	thermal capacitance	J/°C
Rint	internal resistance	Ω
Rth	thermal resistance	°C/W
I	battery current	A
T	battery temperature	°C
Tamb	ambient temperature	°C

References

[1] Alireza Khaligh, and Michael D'Antonio, "Global Trends in High-Power Onboard Chargers for Electric Vehicles," *IEEE Transactions on Vehicular Technology*, vol. 68, no. 4, pp. 3306-3324, 2019. [CrossRef] [Google Scholar] [Publisher Link]

[2] Md Safayatullah et al., "A Comprehensive Review of Power Converter Topologies and Control Methods for Electric Vehicle Fast Charging Applications," *IEEE Access*, vol. 10, pp. 40753-40793, 2022. [CrossRef] [Google Scholar] [Publisher Link]

[3] Sithara S.G. Acharige et al., "Review of Electric Vehicle Charging Technologies, Standards, Architectures, and Converter Configurations," *IEEE Access*, vol. 11, pp. 41218-41255, 2023. [CrossRef] [Google Scholar] [Publisher Link]

[4] Rajendra Kumar Prajapati, and Rohit Kumar, "Review on Advancements in Bidirectional On-Board Chargers for Electric Vehicles," *2024 IEEE 11th Power India International Conference (PIICON)*, Jaipur, India, pp. 1-6, 2024. [CrossRef] [Google Scholar] [Publisher Link]

[5] Mohamed Y. Metwly et al., "A Review of Integrated On-Board EV Battery Chargers: Advanced Topologies, Recent Developments and Optimal Selection of FSCW Slot/Pole Combination," *IEEE Access*, vol. 8, pp. 85216-85242, 2020. [CrossRef] [Google Scholar] [Publisher Link]

[6] Sohit Sharma, Mohan V. Aware, and Apekshit Bhowate, "Integrated Battery Charger for EV by using Three-Phase Induction Motor Stator Windings as Filter," *IEEE Transactions on Transportation Electrification*, vol. 6, no. 1, pp. 83-94, 2020. [CrossRef] [Google Scholar] [Publisher Link]

[7] Jyoti Gupta, Rakesh Maurya, and Sabha Raj Arya, "Improved Power Quality On-Board Integrated Charger with Reduced Switching Stress," *IEEE Transactions on Power Electronics*, vol. 35, no. 10, pp. 10810-10820, 2020. [CrossRef] [Google Scholar] [Publisher Link]

[8] V. Vidya, and R. Sudharshan Kaarthik, "Modeling and Control of an Integrated Battery Charger with Split-Phase Machine," *IEEE Transactions on Industry Applications*, vol. 57, no. 2, pp. 1588-1597, 2021. [CrossRef] [Google Scholar] [Publisher Link]

[9] Jaime Pando-Acedo et al., "Improved Three-Phase Integrated Charger Converter Connected to Single-Phase Grid with Torque Cancellation," *IEEE Access*, vol. 9, pp. 108266-108275, 2021. [CrossRef] [Google Scholar] [Publisher Link]

[10] Yosuke Ito, and Hitoshi Haga, "Reduction of Torque Vibration in Integrated Onboard Chargers using Stator Windings of an IPMSM," *IEEJ Journal of Industry Applications*, vol. 12, no. 5, pp. 982-989, 2022. [CrossRef] [Google Scholar] [Publisher Link]

[11] Yanxiong Lei et al., "High-Power-Density EV Integrated Fast Battery Chargers based on the General Torque-Cancellation Law for Three-Phase Motors," *CSEE Journal of Power and Energy Systems*, vol. 10, no. 2, pp. 756-766, 2024. [CrossRef] [Google Scholar] [Publisher Link]

[12] Minghao Tong et al., "An Onboard Two-Stage Integrated Fast Battery Charger for EVs based on a Five-Phase Hybrid-Excitation Flux-Switching Machine," *IEEE Transactions on Industrial Electronics*, vol. 68, no. 2, pp. 1780-1790, 2021. [CrossRef] [Google Scholar] [Publisher Link]

[13] Paolo Pescetto et al., "Galvanically Isolated On-Board Charger Fully Integrated with 6-Phase Traction Motor Drives," *IEEE Access*, vol. 11, pp. 26059-26069, 2023. [CrossRef] [Google Scholar] [Publisher Link]

[14] Kai Zhou, Haolin Fang, and Yang Liu, "Driving-Charging Integrated Controller for Electric Vehicles," *IEEE Access*, vol. 10, pp. 66545-66563, 2022. [CrossRef] [Google Scholar] [Publisher Link]

[15] Kai Zhou, Yuhe Che, and Haolin Fang, "Research on Motor Driving and Vehicle Charging Integrated System," *Electrical Engineering*, vol. 106, no. 5, pp. 5431-5445, 2024. [CrossRef] [Google Scholar] [Publisher Link]

[16] Arun Jose, and Sonam Shrivastava, "Evolution of Electric Vehicles, Battery State Estimation, and Future Research Directions: A Critical Review," *IEEE Access*, vol. 12, pp. 158627-158646, 2024. [CrossRef] [Google Scholar] [Publisher Link]

[17] Maryam Alizadeh et al., "Driving-Aware Battery Thermal-Management System in Electric Vehicles: Incorporating Cell Discharge Rate, Temperature, and Aging," *IEEE Transactions on Transportation Electrification*, vol. 11, no. 3, pp. 8260-8270, 2025. [CrossRef] [Google Scholar] [Publisher Link]

[18] Jingang Han et al., "A Three-Phase Bidirectional Grid-Connected AC/DC Converter for V2G Applications," *Journal of Control Science and Engineering*, vol. 2020, no. 1, pp. 1-12, 2020. [CrossRef] [Google Scholar] [Publisher Link]